

# Metabolism of Scoparone in Experimental Animals and Humans

**DOI** 10.1055/a-0835-2301
Planta Med 2019; 85: 453–464



**Publishing House and Copyright:**
© 2019 by
Georg Thieme Verlag KG
Rüdigerstraße 14
70469 Stuttgart
ISSN 0032-0943



Thieme

Thieme

# Metabolism of Scoparone in Experimental Animals and Humans

Authors
Risto O. Juvonen[1], Filip Novák[2], Eleni Emmanouilidou[3], Seppo Auriola[1], Juri Timonen[1], Aki T. Heikkinen[4], Jenni Küblbeck[1], Moshe Finel[5], Hannu Raunio[1]

Affiliations
1 School of Pharmacy, Faculty of Health Sciences, University of Eastern Finland, Kuopio, Finland
2 Department of Biochemical Sciences, Faculty of Pharmacy, Charles University, Hradec Králové, Czech Republic
3 School of Pharmacy, Faculty of Health Sciences, Aristotle University of Thessaloniki, Thessaloniki, Greece
4 Admescope Ltd, Oulu, Finland
5 Division of Pharmaceutical Chemistry and Technology, Faculty of Pharmacy, University of Helsinki, University of Helsinki, Finland

Key words
scoparone, isoscopoletin, scopoletin, esculetin, CYP, UGT

received November 9, 2018
revised January 2, 2019
accepted January 16, 2019

Bibliography
DOI https://doi.org/10.1055/a-0835-2301
Published online February 8, 2019 | Planta Med 2019; 85: 453–464 © Georg Thieme Verlag KG Stuttgart · New York | ISSN 0032-0943

Correspondence
Professor Risto O. Juvonen
School of Pharmacy, Faculty of Health Sciences,
University of Eastern Finland
Yliopistonranta 1C, 70210 Kuopio, Finland
Phone: + 35 84 07 28 26 99, Fax: + 35 8 17 16 24 24
risto.juvonen@uef.fi

Supporting information available online at
http://www.thieme-connect.de/products

## ABSTRACT

Scoparone, a major constituent of the Chinese herbal medicine Yin Chen Hao, expresses beneficial effects in experimental models of various diseases. The intrinsic doses and effects of scoparone are dependent on its metabolism, both in humans and animals. We evaluated in detail the metabolism of scoparone in human, mouse, rat, pig, dog, and rabbit liver microsomes *in vitro* and in humans *in vivo*. Oxidation of scoparone to isoscopoletin via 6-O-demethylation was the major metabolic pathway in liver microsomes from humans, mouse, rat, pig and dog, whereas 7-O-demethylation to scopoletin was the main reaction in rabbit. The scoparone oxidation rates in liver microsomes were 0.8–1.2 µmol/(min*g protein) in mouse, pig, and rabbit, 0.2–0.4 µmol/(min*g protein) in man and dog, and less than 0.1 µmol/(min*g) in rat. In liver microsomes of all species, isoscopoletin was oxidized to 3-[4-methoxy-ρ-(3, 6)-benzoquinone]-2-propenoate and esculetin, which was formed also in the oxidation of scopoletin. Human CYP2A13 exhibited the highest rate of isoscopoletin and scopoletin oxidation, followed by CYP1A1 and CYP1A2. Glucuronidation of isoscopoletin and scopoletin was catalyzed by the human UGT1A1, UGT1A6, UGT1A7, UGT1A8, UGT1A9, UGT1A10, and UGT2B17. Dog was most similar to man in scoparone metabolism. Isoscopoletin glucuronide and sulfate conjugates were the major scoparone *in vivo* metabolites in humans, and they were completely excreted within 24 h in urine. Scoparone and its metabolites did not activate key nuclear receptors regulating CYP and UGT enzymes. These results outline comprehensively the metabolic pathways of scoparone in man and key preclinical animal species.

## Introduction

Scoparone (6,7-dimethoxy-2H-chromen-2-on) is a coumarin derivative that is present in multiple plants, especially *Artemisia capillaris* Thunb (Asteraceae). Scoparone is the major active component in the Chinese herbal medicine Yin Chen Hao, which is used to produce several other traditional Chinese medicine products. Yin Chen Hao has been used to treat various diseases, especially hepatic disorders such as liver cirrhosis, liver cancer, jaundice, and cholecystitis [1–3]. Scoparone has various pharmacological effects in experimental models, including hepatoprotective [2], renoprotective [4], vasorelaxant [5, 6], anticarcinogenic, antioxidant, and anti-inflammatory [7–12] properties.

Recent studies have evaluated the mechanisms of these actions. A metabolomics study suggested that the hepatoprotective effects of scoparone on liver injury in rats are associated with regulated expression of proteins that are involved in antioxidation and signal transduction, energy production, immunity, metabolism, and chaperoning [13]. Another study, using lipidomics techniques, revealed substantial scoparone-induced changes in lipid

**ABBREVIATIONS**

| | |
|---|---|
| AhR | aryl hydrocarbon receptor |
| CAR | constitutive androstane receptor |
| CYP | cytochrome P450 |
| LBD | ligand-binding domain |
| MBQP | 3-[4-methoxy-ρ-(3, 6)-benzoquinone]-2-propenoate |
| PAPS | 3′-phosphoadenosine-5′-phosphosulfate |
| PCN | pregnenolone 16α-carbonitrile |
| PXR | pregnane X receptor |
| rCAR | rat CAR |
| UDP | uridine diphosphate |
| UGT | UDP-glucuronosyltransferase |

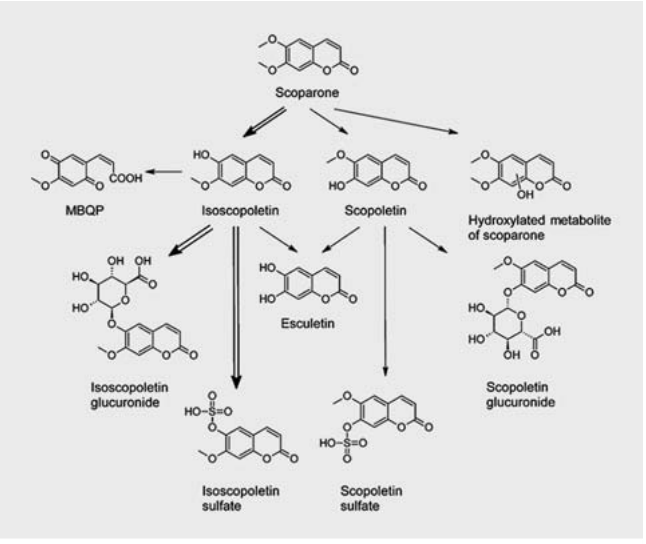


▶ **Fig. 1** Metabolic pathways of scoparone. The major metabolic reactions in human are indicated by double lines arrows.

metabolism in mouse primary hepatocytes [14]. Scoparone significantly inhibited the proliferation and activation of hepatic stellate cells through inactivation of the TGF-b/Smad signaling pathway [15]. Some of the hepatic effects of scoparone appear to be mediated by activation of the constitutive androstane receptor (CAR) [16, 17].

Although being increasingly investigated, there is still very limited knowledge about the chemical compositions, pharmacokinetics, pharmacodynamics, and metabolomics of herbal medicines [18, 19]. In addition, it is well known that there are substantial interspecies differences in their pharmacokinetics due to differences in metabolic enzymes [20]. Extrapolation of metabolism data from animals to human is therefore challenging. The available data on scoparone pharmacokinetics is limited. In the rat, orally administered scoparone is rapidly absorbed and is distributed in the extravascular system but not in the brain [21]. Scoparone in vitro metabolism has been reported to be 7–10 times faster in the hamster and monkey primary hepatocytes than in the rat ones [22]. The scopoletin/isoscopoletin ratio also differs between species, indicating different oxidation pathways [23].

The metabolic pathways of scoparone are illustrated in ▶ **Fig. 1**. CYP enzymes catalyze oxidation of scoparone to scopoletin and isoscopoletin by 7- and 6-O-demethylation reactions, respectively, in rat, mouse, and hamster. Scopoletin and isoscopoletin are further oxidized to esculetin, while isoscopoletin is converted to 3-[4-methoxy-ρ-(3,6)-benzoquinone]-2-propenoate (MBQP) [22–25]. Isofraxidin, an 8-methoxy derivative of scopoletin, is a minor metabolite of scoparone in rat [26]. In mice, the CYP2C29 enzyme catalyzes oxidative hydrolysis of isoscopoletin to MBQP [27]. In humans, CYP1A2 was shown to oxidize scoparone to scopoletin [22]. Recently we showed that the human extrahepatic CYP1A1 and CYP2A13 were more efficient catalysts for this reaction than the hepatic CYP1A2 [28]. The rate of *in vitro* liver microsomal scoparone 7-O-demethylation is lower in humans than in pig, mouse, and rabbit. These results suggested that mouse, rat, pig, and rabbit are not suitable surrogate species for evaluating scoparone pharmacokinetics in humans [28].

The aim of this study was to comprehensively evaluate the metabolism of scoparone in experimental animals and humans. To achieve this, (1) a HPLC-MS method was developed to accurately determine the metabolites of scoparone; (2) oxidation and glucuronidation of scoparone and its main metabolites were determined in liver microsomes of human and 5 preclinical species; and (3) *in vivo* metabolism of scoparone was determined in 2 human subjects by measuring urinary metabolites after oral dosing.

## Results

A HPLC-MS method was established to analyze scoparone and its metabolites (▶ **Fig. 2**, **Table 1**, **Fig. 1S**, Supporting Information). Accurate quantification was possible for scoparone, scopoletin, isoscopoletin, and esculetin based on peak area in HPLC-MS chromatograms. Qualitative standards for the glucuronides and sulfonates of scopoletin and isoscopoletin were produced by biosynthesis (see Materials and Methods). Standards for MBQP and the other hydroxylation metabolites were not available, and their identification was based on their accurate m/z value and specific fragmentation peaks. The oxidation and glucuronidation rates of scopoletin were determined by measuring the decrease of its fluorescence intensity (**Fig. 2S**, Supporting Information).

Scoparone oxidation was measured in liver microsomes of different species. Scoparone 6-O-demethylation to isoscopoletin was the major oxidation reaction product in microsomes from human, pig, dog, mouse, and rat. In rabbit, the major pathway was via scoparone 7-O-methylation to scopoletin (▶ **Fig. 1** and **3**). The ratio isoscopoletin/scopoletin was about 10 in human, pig, and dog, 2–3 in mouse and rat, and only 0.1–0.5 in rabbit (▶ **Fig. 3 A**). In pig and mouse, microsomes a substantial amount of MBQP was formed from scoparone, based on the peak area (▶ **Fig. 1**, **Table 1**). MBQP was not detected in the other species. Small amounts of 2 hydroxylated scoparone metabolites (M5 and M6) was observed in human, pig, mouse, rabbit, and dog (▶ **Fig. 1**, **Table 1**). The highest rate of scoparone oxidation was exhibited by mouse, pig, and rabbit liver microsomes, followed by an intermediate rate

(20–40 %) in human and dog microsomes, and down to rat (less than 5 %), the lowest rate among the species investigated (▶ **Fig. 3 B**). Oxidation of scoparone was faster to isoscopoletin than to scopoletin in human, pig, mouse, rat, and dog, while in rabbit the formation of scopoletin was faster than that of isoscopoletin (▶ **Fig. 3 C** and **D**).

Oxidation of isoscopoletin and scopoletin *in vitro* was evaluated next. Isoscopoletin was oxidized to esculetin via the 7-O-demethylation reaction and also partly to MBQP. Oxidation to MBQP was faster than to esculetin, although precise quantitation of MBQP formation was not possible due to the lack of a suitable standard. The rate of isoscopoletin-7-O-demethylation was significantly lower than the rate of isoscopoletin oxidation (less than 50 %, data not shown). The rate of isoscopoletin 7-O-demethylation was highest in rat and lowest in human and pig liver microsomes (▶ **Fig. 4 A**). The oxidation of isoscopoletin to MBQP was 3–20 times faster in mouse, pig and rabbit than in dog, rat or human liver microsomes (▶ **Fig. 4 B**). Only human CYP1A1 catalyzed significantly isoscopoletin 7-O-demethylation to esculetin (▶ **Fig. 4 C**), while CYP1A1, CYP1A2 and CYP2A13 oxidized isoscopoletin to MBQP efficiently (▶ **Fig. 4 D**).

Scopoletin 6-O-demethylation reaction transforms the strongly fluorescent scopoletin to the weakly fluorescent esculetin, allowing the use of fluorescence decrease to determine oxidation rate (**Fig. 2S**, Supporting Information). This reaction was catalyzed faster in liver microsomes from humans, mouse and pig than in rabbit, dog, and rat microsomes (▶ **Fig. 5 A**). Human CYP2A13 catalyzed the reaction 7–26 times faster than CYP1A1, CYP1A2, CYP2C9, and CYP3A4 (▶ **Fig. 5 B**). Pretreatment of rats and mice with CYP inducing agents (phenobarbital, pyrazole, PCN, *β*-naphthoflavone) increased the oxidation rate (▶ **Fig. 5 C** and **D**).

Glucuronidation of scopoletin and isoscopoletin was assessed *in vitro*. Isoscopoletin glucuronidation took place at the highest rate in pig liver microsomes (1.07 ± 0.24 µmol/[min*g protein]), followed by rabbit (70 % vs. pig), mouse (64 %), human (42 %), dog (18 %), and rat (6 %) liver microsomes (▶ **Fig. 6 A**). UGT1A10 exhibited the highest isoscopoletin glucuronidation rate among the human UGTs, followed by UGT1A9 (50 % vs. 1A10) and UGT1A6 (38 %). UGT1A1, UGT1A7, UGT1A8, and UGT2A1 also catalyzed this reaction, but at very low rates (2–8 %) (▶ **Fig. 6 B**).

The rate of scopoletin glucuronidation was highest in pig liver microsomes, followed by rabbit, human, mouse, dog, and rat microsomes (▶ **Fig. 7 A**). Interestingly, the scopoletin glucuronidation rate was equally high in human liver and intestine microsomes. Among the recombinant human UGTs, UGT1A6 catalyzed the reaction at the highest rate, followed by UGT1A10, UGT1A8, UGT1A7, UGT1A9, UGT2B17, and lastly UGT1A1 (▶ **Fig. 7 B**, **Table 2**). UGT1A9 was a high-affinity enzyme for this reaction, as the $K_m$ value of the other UGTs was at least 6 times higher. The glucuronidation efficiency ($V_{max}/K_m$) varied between 0.083 L/(min*g protein) for UGT1A7 and 0.28 L/(min*g protein) for UGT2B17. Pretreatment of rats with *β*-naphthoflavone and dexamethasone increased scopoletin glucuronidation (▶ **Fig. 7 C**). In mice pretreated with pyrazole, PCN or phenobarbital, scopoletin glucuronidation was not affected (▶ **Fig. 7 D**).

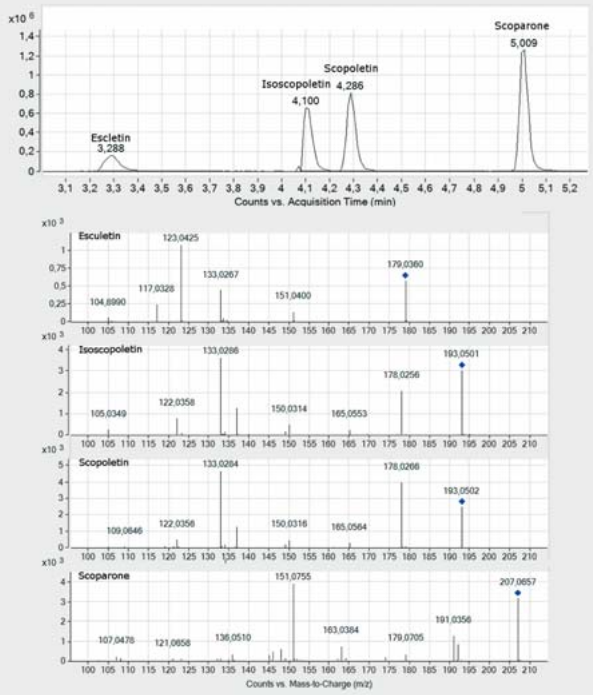


▶ **Fig. 2** An HPLC chromatogram of scoparone and its 3 oxidative metabolites and their fragmentation in MS. The compounds were isolated from urine samples or formed during incubation in the presence of liver microsomes. They were eluted from a Zorbax Eclipse XDB-C18 column by gradient of water-methanol solution containing 0.1 % v/v of formic acid.

In the human *in vivo* study, 5 mg scoparone was taken orally by 2 male volunteers, and urine samples were collected during 24 h. Nine metabolites of scoparone were detected in the urine samples: isoscopoletin, scopoletin, MBQP, 3 glucuronides, and 3 sulfates. Neither parent scoparone nor esculetin were detected, at least under our detection method of accurate mass and MS-fragmentation pattern (▶ **Fig. 8**, **Table 3**). About 40–75 % of the metabolites were excreted to the urine within the first 4 h after ingestion, and excretion was complete in 24 h. The major metabolites in the urine were glucuronides and sulfates of isoscopoletin. The peak areas of the glucuronides and sulfates represented 70–90 % of the total metabolite peak areas. The concentration of unconjugated isoscopoletin in the urine was low, but 10 times more abundant than scopoletin. The peak area of urinary MBQP was small.

Binding activation of nuclear receptors by scoparone and its metabolites were determined. Neither scoparone nor its metabolites activated the studied receptors, while the positive controls elicited robust activations (▶ **Fig. 9**).

MS/MS spectra of scoparone metabolites and data on scopoletin 6-O-demethylation and scopoletin glucuronidation assays are available in the supporting information.

▶ **Table 1** MS characteristics of scoparone and its *in vitro* oxidation metabolites in the positive ionization mode.

| Name | Standard | Calculated mass | Molecular formula | Retention time (min) | Fragment ions | |
|---|---|---|---|---|---|---|
| Scoparone | Yes | 206.0579 | $C_{11}H_{10}O_4$ | 5.01 | 207.0657 | Parent ion |
| | | | | | 191.0356 | ▪ $CH_4$ [1] |
| | | | | | 163.0384 | ▪ $CH_3 - CO$ [1] |
| | | | | | 179.0705 | ▪ CO |
| | | | | | 151.0755 | ▪ CO – CO |
| Isoscopoletin | Yes | 192.0423 | $C_{10}H_8O_4$ | 4.10 | 193.0501 | Parent ion |
| | | | | | 178.0256 | ▪ $CH_3$ [1] |
| | | | | | 150.0314 | ▪ $CH_3 - CO$ [1] |
| | | | | | 133.0286 | ▪ $CH_3 - CO - OH$ [1] |
| Scopoletin | Yes | 192.0423 | $C_{10}H_8O_4$ | 4.29 | 193.0502 | Parent ion |
| | | | | | 178.0266 | ▪ $CH_3$ [1] |
| | | | | | 150.0316 | ▪ $CH_3 - CO$ [1] |
| | | | | | 133.0284 | ▪ $CH_3 - CO - OH$ [1] |
| Esculetin | Yes | 178.0266 | $C_9H_6O_4$ | 3.29 | 179.0360 | Parent ion |
| | | | | | 151.0400 | ▪ CO |
| | | | | | 123.0425 | ▪ CO – CO |
| | | | | | 133.0267 | ▪ CO – H2O |
| MBQP | No | 208.0372 | $C_{10}H_8O_5$ | 3.91 | 209.0443 | Parent ion |
| | | | | | 194.0220 | ▪ $CH_3$ [2] |
| M5 | No | 222.0528 | $C_{11}H_{10}O_5$ | 5.11 | 223.0607 | Parent ion |
| | | | | | 207.0266 | ▪ $CH_3$ [1] |
| | | | | | 162.0314 | ▪ $CH_3 - OH - CO$ |
| M6 | No | 222.0528 | $C_{11}H_{10}O_5$ | 4.88 | No fragmentation, due to low signal | |

[1] reference [26], [2] reference [27]

## Discussion

It is important to know the metabolic pathways of drugs and other xenobiotics, including the constituents of traditional Chinese medicine, since metabolic features directly affect their pharmaco/toxicokinetics, efficacy, and safety. In this study we evaluated the *in vitro* metabolism of scoparone in human, mouse, rat, pig, rabbit, and dog liver microsomes and *in vivo* in humans. The main results were as follows. (1) The major primary metabolite of scoparone in liver microsomes of humans, mouse, rat, dog, and pig is isoscopoletin, whereas in rabbit liver microsomes it is scopoletin. (2) Both isoscopoletin and scopoletin were further metabolized by oxidation and conjugation reactions to secondary metabolites such as MBQP and isoscopoletin glucuronide. (3) There was a good correlation between metabolites that were detected *in vitro* and those formed *in vivo* and excreted to urine in humans. Isoscopoletin glucuronide and sulfate conjugates were the most abundant metabolites in the urine. The primary metabolites isoscopoletin and scopoletin and the secondary metabolite MBQP were minor metabolites in human urine. The parent compound, scoparone, was not found at all in urine.

Scoparone is oxidized to isoscopoletin and scopoletin catalyzed by CYP1A2 in human liver microsomes [22, 28]. However, the extrahepatic enzymes CYP1A1 and CYP2A13 catalyze scoparone oxidation more efficiently than CYP1A2 [28]. The present study confirmed that the main primary metabolite of scoparone is isoscopoletin, as over 10 times more isoscopoletin than scopoletin was formed *in vitro*. Moreover, in the human *in vivo* urine samples, the amounts of isoscopoletin and its glucuronide and sulfate conjugates were at least 10 times more abundant than scopoletin and its conjugates.

Both isoscopoletin and scopoletin were further oxidized to esculetin by demethylation reactions. In addition, isoscopoletin was oxidized to MBQP in human liver microsomes. MBQP was identified earlier as a metabolite of scoparone or isoscopoletin; the reaction is catalyzed by human CYP1A2 [22], mouse CYP2C29 [27], and occurs also in rat liver microsomes [26]. In the present study MBQP was detected in the urine, and recombinant human CYP1A1, CYP1A2, and CYP2A13 catalyzed its formation from isoscopoletin. The urinary concentrations of isoscopoletin and scopoletin were much lower than the concentrations of their respective glucuronide and sulfate conjugates, indicating that these conjugations occur rapidly in the body. Collectively, these results demonstrate that the main metabolic pathway of scoparone in humans is oxidation to isoscopoletin, which is further conjugated to its glucuronide or sulfate conjugates, while a small amount is

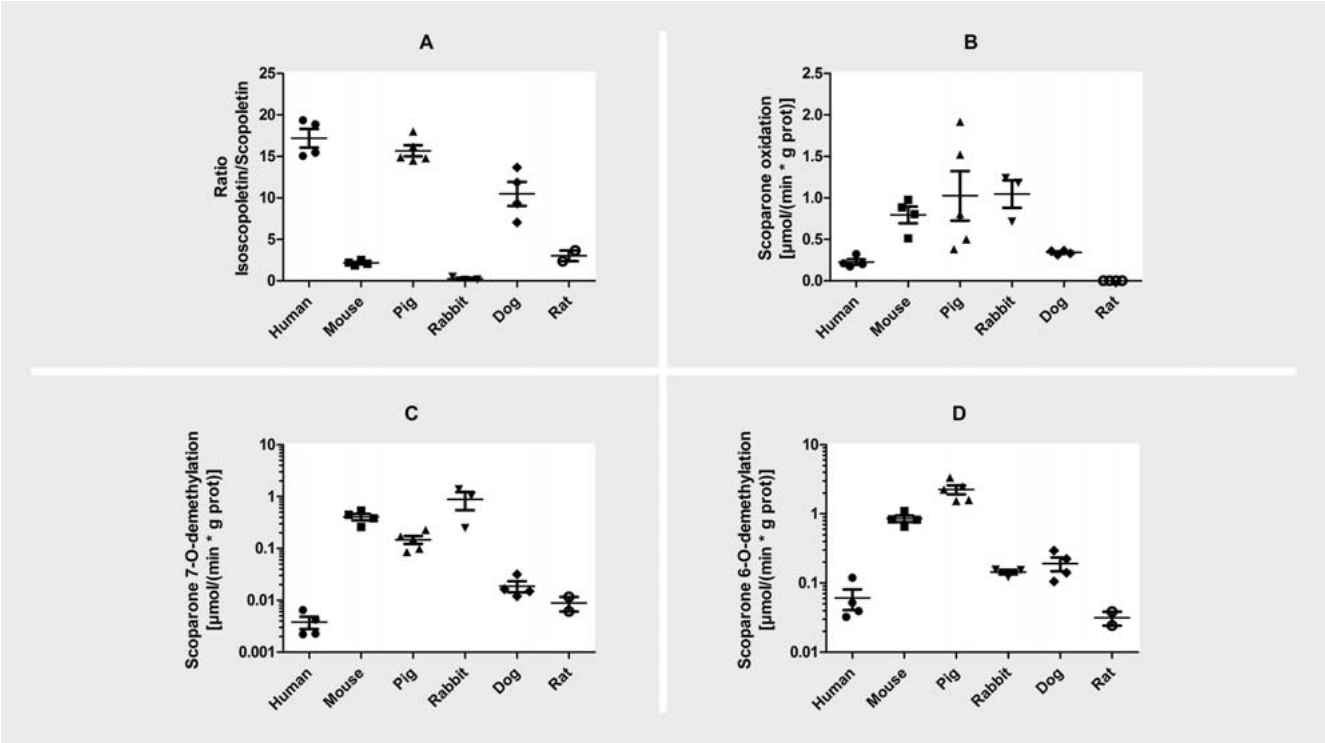


▶ **Fig. 3** *In vitro* oxidation of scoparone in liver microsomes of different species. The incubations were carried out as described in the Materials and Methods section, in the presence of 10 µM scoparone. Panel **A** shows the ratio of isoscopoletin/scopoletin, panel **B** the oxidation rate of scoparone, panel **C** scoparone 7-O-demethylation rate, and panel **D** scoparone 6-O-demethylation rate. The human samples were from 1 individual donor and commercial pooled samples. The pig, rabbit, and dog samples were from individual animals. The rat and mouse samples were pooled liver microsomes. The symbols indicate the number of samples and whiskers indicate the standard errors of means.

oxidized to MBQP. These metabolites were observed in urine; other possible excretion routes were not evaluated in this study. Esculetin or its conjugates were not present in urine in the human experiment.

Isoscopoletin oxidation by CYP1A1 and CYP1A2 differed, as isoscopoletin 7-O-demethylation to esculetin was catalyzed only by CYP1A1, whereas isoscopoletin oxidation to MBQP was catalyzed by both CYP1A1 and CYP1A2, as well as by CYP2A13 (▶ **Fig. 1**). This suggests that isoscopoletin is oriented somewhat differently for oxidation in the active sites of these enzymes. Scopoletin 6-O-demethylation to esculetin was catalyzed efficiently by CYP2A13, which catalyzes also scoparone 7-O-demethylation [28]. In addition, both CYP1A1 and CYP1A2 catalyze the reaction, but less efficiently. It may be concluded that oxidation of scoparone and its primary metabolites are catalyzed by hepatic CYP1A2 and extrahepatic CYP1A1 and CYP2A13.

The efficient *in vivo* conjugation of isoscopoletin and scopoletin in humans was probably due to their conjugation by several UGT enzymes. Multiple UGTs including UGT1A1, 1A6, 1A7, 1A8, 1A9, and 1A10 catalyzed glucuronidation of both compounds. However, the hepatic UGT1A6 was the most efficient catalyst for scopoletin glucuronidation and the extrahepatic UGT1A10 for isoscopoletin glucuronidation. UGT2B17, expressed both in the small intestine and the liver, catalyzed glucuronidation of scopoletin. Earlier, scopoletin has been used as a nonspecific substrate for UGT1A3, UGT1A6, and UGT1A9 [29]. In this study we did not observe scopoletin glucuronidation by UGT1A3. The reason may be that the $K_m$ value for UGT1A3 catalyzed scopoletin glucuronidation is 500 µM, whereas 10 µM scopoletin was used in the present study.

Scoparone, scopoletin and isoscopoletin did not activate the human, mouse, and rat nuclear receptors CAR and PXR or AhR. It can thus be predicted that scoparone and its metabolites, in these species, do not activate these nuclear receptors *in vivo* and would not exert biological effects in this mechanism. It was previously reported that the activation of human CAR mediates some of the hepatic effects of scoparone [16, 17]. These studies were mainly done by using full-length receptor and natural promoters and/or by studying the impact of the compound(s) on the expression of human CAR target genes. As our assays measured directly activation of the nuclear receptors as a result of the test compound binding to the nuclear receptor ligand binding domain, indirect "phenobarbital-like" activation would not be detected. This might explain the discrepancy in results in comparison with the previous studies.

A summary of 6 parameters related to the metabolism of scoparone in different species is in ▶ **Table 4**. The advantage of *in vivo* animal models in comparison with *in vitro* models is that they mimic better all the steps, from oral exposure to the actual outcome. In addition, an estimation of the effective dose, instead of an *in vitro* concentration, is obtained. However, when extrapolating data to humans, it is important that the kinetics and metabo-

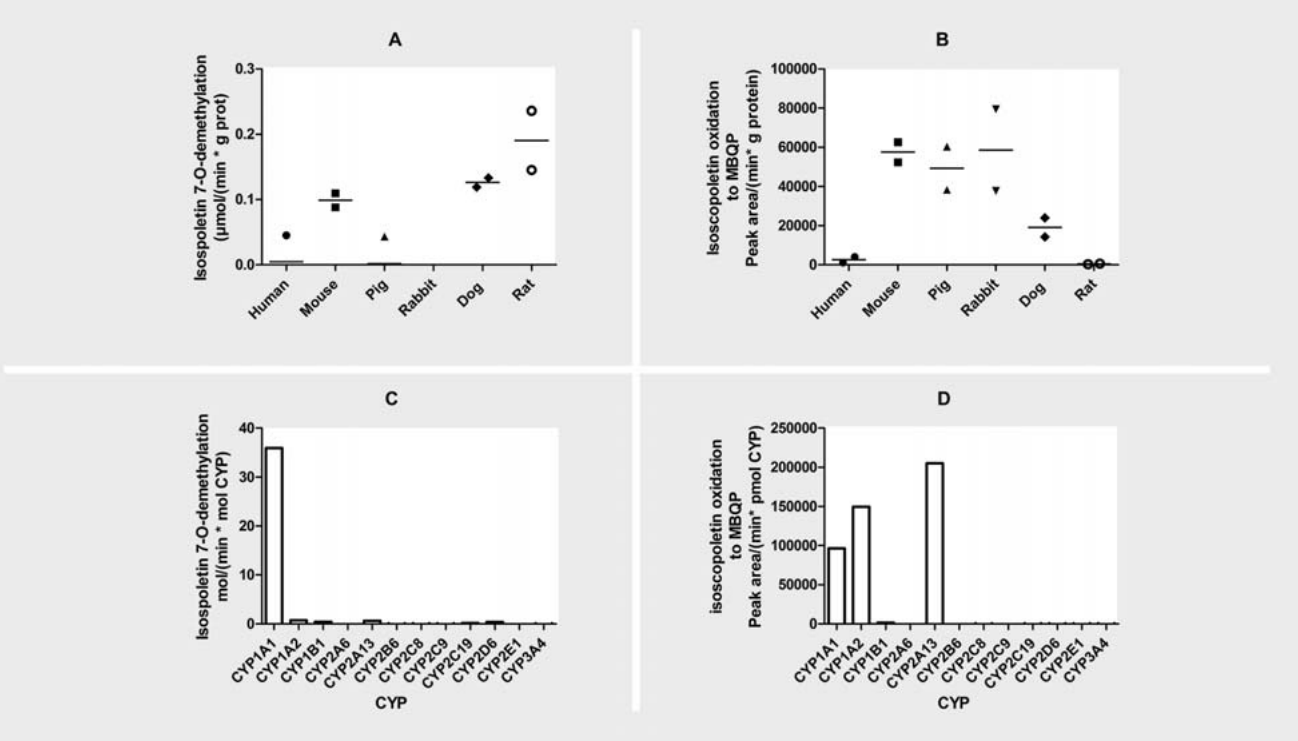


▶ **Fig. 4** *In vitro* oxidation of isoscopoletin. The assay conditions and analyses by HPLC-accurate MS were as described in the Materials and Methods section. Incubation mixture contained 10 µM isoscopoletin. Panels **A** and **B** show the oxidation rate of isoscopoletin to esculetin or to MBQP by liver microsomes, while panels **C** and **D** present the rates of individual human CYP enzymes. The bars indicate averages of 2 duplicate samples.

lism in the selected animal are as similar as possible to the human situation. In this study, clear similarities in scoparone metabolism *in vitro* were found between dog and humans, while the metabolism in rat was least similar (▶ **Table 4**). In particular, the oxidation rate of scoparone, as well as the isoscopoletin/scopoletin ratio and the glucuronidation rate of scopoletin in dog liver microsomes were similar to those in humans.

A special feature in human scoparone metabolism is that the extrahepatic CYP2A13 and CYP1A1 are more efficient catalysts than the hepatic CYP1A2 [28]. This was reflected as relatively slow elimination of scoparone metabolites into urine. Coumarin, a very similar substance to scoparone is eliminated much faster, because hepatic CYP2A6 oxidizes it efficiently to 7-hydroxycoumarin, which is further conjugated to glucuronide and excreted [30]. Coumarin metabolism is similar among certain mouse strains and humans, whereas in rat it is very different [31, 32]. When it comes to scoparone, however, this study suggests that dog would be the best model and mouse better than rat to study its *in vivo* effects, based on metabolic similarity.

## Materials and Methods

### Chemicals

Tris-HCl, $MnCl_2$, $MgCl_2$, isocitric acid, isocitric acid dehydrogenase, scopoletin (99% purity), esculetin (98% purity), scoparone (98% purity), UDP-glucuronic acid, and PAPS were purchased from Sigma-Aldrich. Acetonitrile (Ultra gradient HPLC-grade), $MgCl_2$ (> 99% purity), and KCl (> 99% purity) were from J. T. Baker, NADPH and NADP were from Roche Diagnostics, and isoscopoletin (95% purity) from ABCR GmbH & CoKG. Methanol was purchased from Honeywell Riedel-de Haen and formic acid from Honeywell Fluka. All other chemicals were of the highest purity available. The NADPH regenerating system (200 mL) contained 178.5 mg NADP (nicotinamide adenine dinucleotide phosphate), 645 mg isocitric acid, 340 mg KCl, 240 mg $MgCl_2$, 0.32 mg $MnCl_2$, and 15 U isocitric acid dehydrogenase.

### Biological material

The human liver tissue for this study was obtained from the University Hospital of Oulu (Oulu, Finland) as a surplus from organ transplantation surgery. Collection of surplus tissue samples was approved by the Ethics Committee of the Medical Faculty of the University of Oulu (January 21, 1986). After surgical excision, the liver samples were immediately transferred to ice, cut into pieces, snap frozen in liquid nitrogen, and stored at − 80 °C until preparation of microsomes. Human liver microsomes were also purchased from BD Biosciences Discovery Labware.

Pig liver samples were collected from 8-mo old female pigs that were used for practicing surgical procedures at the Kuopio University. DBA/2N/Kuo mice (20–25 g) and Wistar rats (200–300 g) were obtained from the National Laboratory Animal Centre, Kuopio University. Beagle dog liver microsomes were prepared from tissue samples collected at F. Hoffmann-La Roche Ltd (Nutley, NJ) as described earlier [33].

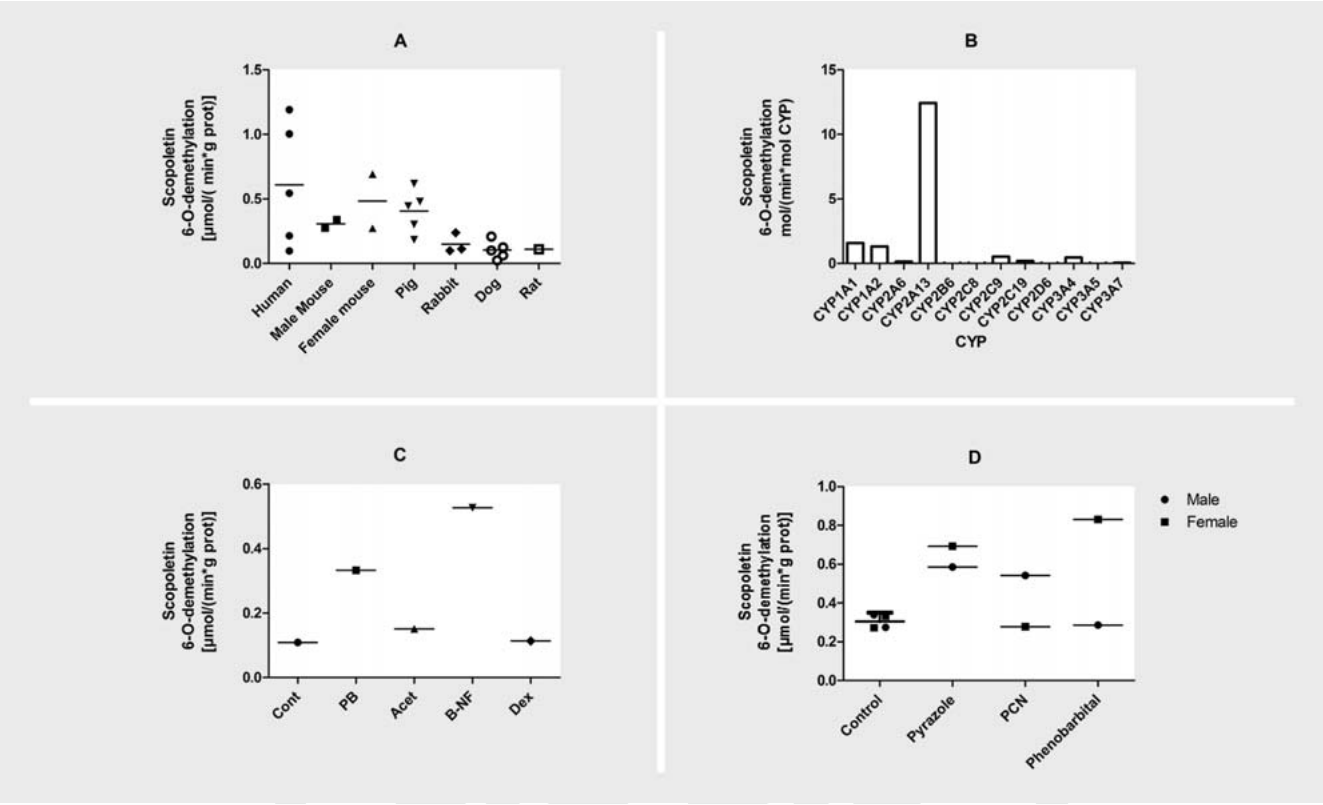


▶ **Fig. 5** *In vitro* scopoletin oxidation rates. The assay was done as described in the Method section, in the presence of 10 µM scopoletin, and was followed by scopoletin fluorescence decrease up to 40 min. Panel **A** shows the rate of scopoletin 6-O-demethylation by liver microsomes. The symbols indicate the number of samples and whiskers indicate the standard errors of means. Panel **B** presents the activity of individual human CYP enzymes. Panel **C** shows the effects of pretreated rats with either phenobarbital (PB), acetone (Acet), *β*-naphthoflavone (B-NF), or dexamethasone (Dex) on the activity measured in pooled microsomes. Panel **D** shows the effect of pretreating mice, either male or female, with pyrazole, PCN, or phenobarbital on the activity of their pooled liver microsomes. The results are averages of duplicate samples (**B, C, D**).

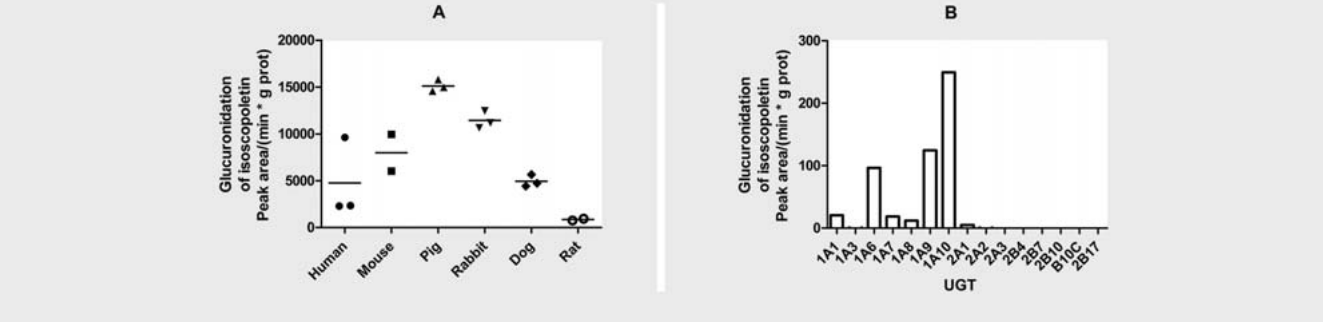


▶ **Fig. 6** *In vitro* glucuronidation of isoscopoletin. The assays and analyses were done as described in the Materials and Methods section, in the presence of 10 µM isoscopoletin. Panel **A** shows the rate of isoscopoletin glucuronidation by liver microsomes from different species and panel **B** by recombinant human UGT enzymes. The results are averages of duplicate samples.

To induce specific CYP forms, rats were pretreated with dexamethasone, *β*-naphthoflavone, acetone, or phenobarbital. DBA/2 mice were pretreated with pyrazole, PCN, or phenobarbital. Details of the treatments have been published earlier [28]. The Ethics Committee for Animal Experiments, University of Kuopio, approved these experiments (Document 01–38, June 1, 2000). Animals were killed 24 h after the last treatment and liver samples were prepared as described below.

Tissue samples were thawed, weighted, chopped into small pieces, and homogenized in 100 mM Tris-HCL buffer, pH 7.4, containing 1 mM $K_2$-EDTA. The supernatants (cytosolic fractions) and pellet (microsomal fractions) were separated by centrifugation. The microsomal fractions were re-homogenized in 100 mM Tris-HCl buffer, pH 7.4, containing 1 mM $K_2$-EDTA and 20% glycerol. Protein concentrations were determined by the Bicinchonic acid

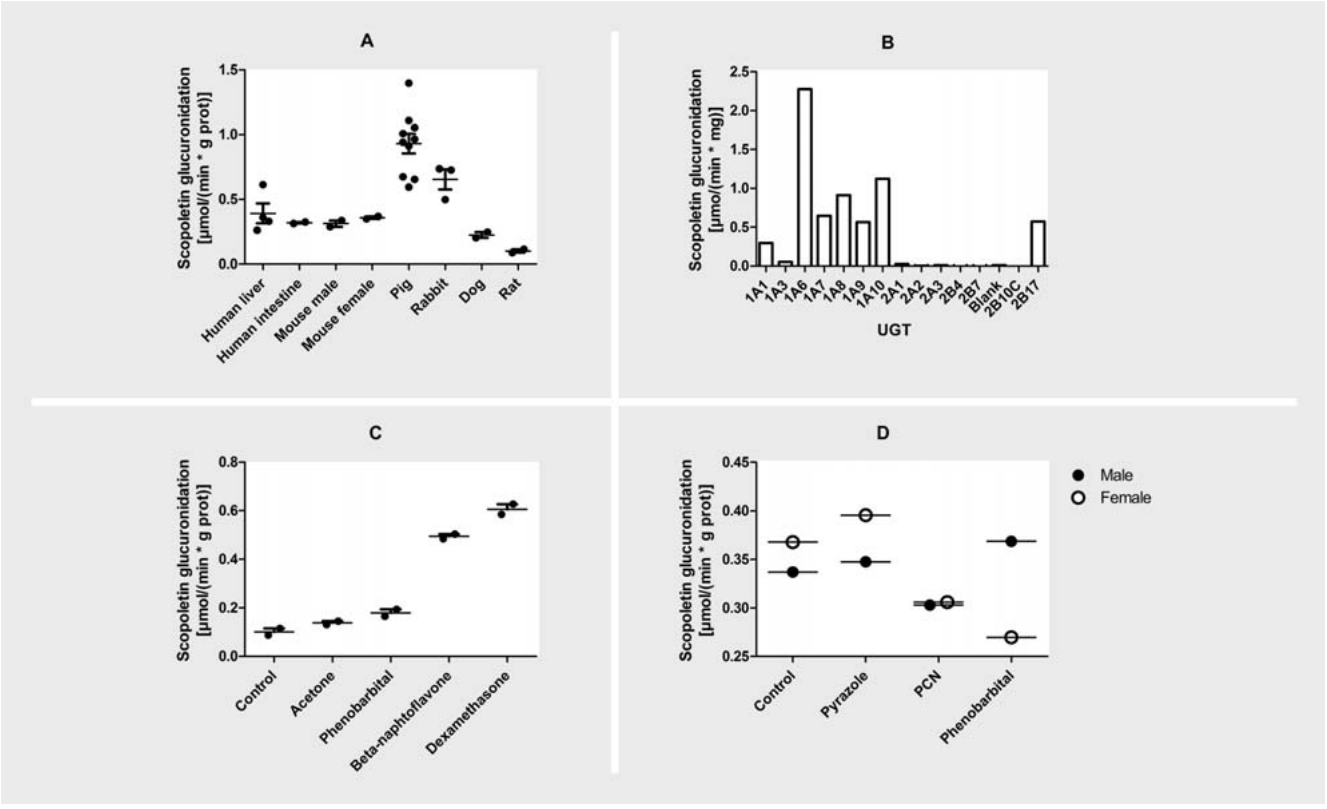


▶ **Fig. 7** *In vitro* glucuronidation of scopoletin. The assays and analyses were done as described in the Materials and Methods section, in the presence of 10 µM scopoletin. Panel **A** shows the rate of scopoletin glucuronidation by liver microsomes and, in the human case, also intestinal microsomes. Glucuronidation by individual recombinant human UGT enzymes are shown in panel **B**. Panels **C** and **D** present the effects of pretreatments of rats (**C**) and mice (**D**) on the scopoletin glucuronidation activity, including a comparison between males to females in the case of mice (panel **D**). The results are averages of duplicate (**B**, **C**, **D**) or more (**A**) samples.

▶ **Table 2** Kinetic values of scopoletin glucuronidation reaction by human UGT enzymes.

| UGT | $K_m$ of scoparone (95% confidence interval) µM | $V_{max}$ (95% confidence interval) µmol/(min*g protein) | $V_{max}/K_m$ L/(min * g protein) |
|---|---|---|---|
| 1A6 | Could not be determined | Could not be determined | |
| 1A7 | 30 (23–37) | 3.8 (3.3–4.3) | 0.13 |
| 1A8 | 24 (16–32) | 2.0 (1.7–2.4) | 0.083 |
| 1A9 | 2.4 (0.6–4.1) | 0.5 (0.40–0.59) | 0.21 |
| 1A10 | 56 (41–72) | 11.2 (9.2–13.3) | 0.20 |
| 2B17 | 17 (12–22) | 4.8 (4.1–5.4) | 0.28 |

Assay (Pierce Biotechnology). The samples were stored at − 80 °C until used.

Baculovirus-infected insect cell-expressed human CYP1A1, 1A2, 2A6, 2A13, 2B6, 2C8, 2C9, 2C19, 2D6, 2E1, 3A4, 3A5, and 3A7 were purchased from BD Biosciences Discovery Labware and used according to the manufacturer's instructions.

Recombinant human UGTs 1A1, 1A3, 1A6, 1A7, 1A8, 1A9, 1A10, 2A1, 2A2, 2A3, 2B4, 2B10, 2B7, and 2B17 were produced, as His-tagged proteins, in baculovirus-infected insect cells as previously described [34–36]. The relative expression level of each of these recombinant UGTs was evaluated by immunodetection, using monoclonal antibody against the His-tag, as described elsewhere [37]. A numerical value of 1.0 was given to the expression level of UGT1A8 and the relative expression level of each of the other UGTs was related to this value. Normalized activities were obtained by dividing the glucuronidation rates by the relative expression level of the tested UGT. In addition, UGTs 1A4, 2B10, and 2B15, also expressed in insect cells, were purchased from Corning Life Sciences. The expression levels of the UGTs in the commercial samples could not be determined, so their protein concentration was used to evaluate reaction rates.

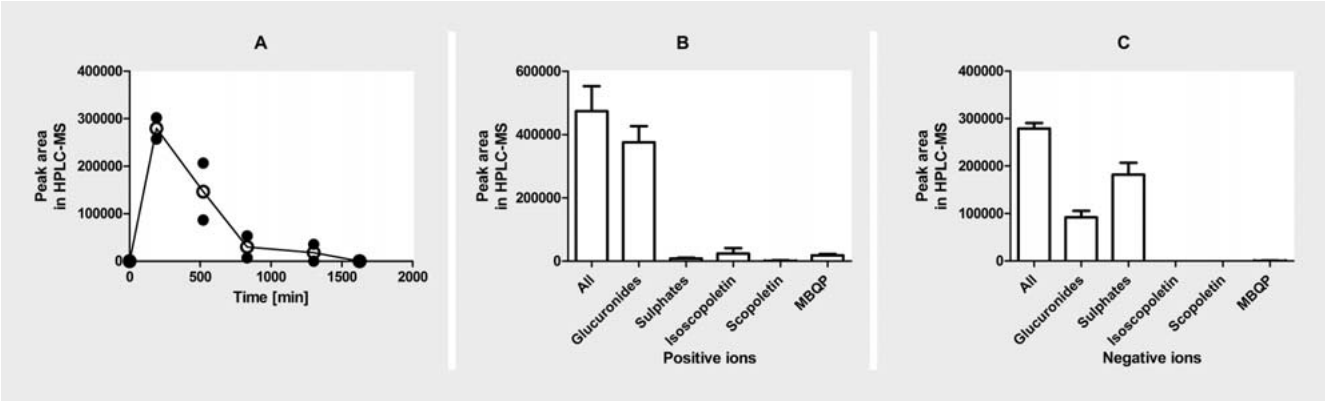


▶ **Fig. 8** Excretion of scoparone and its metabolites into human urine *in vivo*. The experiment and analysis were done as described in the Materials and Methods section. Panel **A** shows the combined peak area of all metabolites at the positive ionization mode. Panels **B** and **C** show the combined peak areas of all metabolites and indicated individual metabolites at positive or negative ionization modes, respectively.

▶ **Table 3** Urine metabolites of scoparone. GA: glucuronic acid; $CH_3$: methyl; $SO_3$: sulfone.

| Name | Molecular formula | Retention time (min) | Fragments in negative ionization mode | Fragments in positive ionization mode | Loss from parent ion |
|---|---|---|---|---|---|
| Isoscopoletin | $C_{10}H_8O_4$ | 4.11 | No fragmentation | | |
| Scopoletin | $C_{10}H_8O_4$ | 4.29 | No fragmentation | | |
| MBQP | $C_{10}H_8O_5$ | 3.93 | No fragmentation | | |
| Isoscopoletin glucuronide (M7) | $C_{16}H_{16}O_{10}$ | 2.89 | 191.0343 | | GA |
| | | | 176.0122 | | GA + $\cdot CH_3$ |
| | | | | 193.0482 | GA |
| | | | | 178.0285 | GA + $\cdot CH_3$ |
| Scopoletin glucuronide (M8) | $C_{16}H_{16}O_{10}$ | 3.04 | No fragmentation | | |
| Isoscopoletin sulfate (M9) | $C_{10}H_8O_7S$ | 3.06 | 191.0344 | | $SO_3$ |
| | | | 176.0114 | | $SO_3$ + $\cdot CH_3$ |
| | | | 148.0170 | | $SO_3$ + $\cdot CH_3$ + CO |
| Scopoletin sulfate (M10) | $C_{10}H_8O_7S$ | 3.27 | No fragmentation | | |
| M11 | $C_{10}H_8O_7S$ | 3.55 | No fragmentation | | |
| M12 | $C_{16}H_{16}O_{11}$ | 3.54 | No fragmentation | | |

## Oxidation of scoparone, isoscopoletin, or scopoletin

The oxidation of 10 µM scoparone and isoscopoletin were carried out at 37 °C in a total volume of 100 µL, in the presence of 100 mM Tris-HCl buffer (pH 7.4), 2 µM CYP or 0–0.2 g/L control microsomal protein and a NADPH regenerating system. The blank reactions lacked either substrate, scoparone or isoscopoletin, enzyme, or NADPH. Samples were incubated for 30 min at 37 °C, and the reaction was stopped by the addition of 300 µL acetonitrile and centrifugation for 5 min 10 000 *g*. The supernatant was stored at − 80 °C and analyzed by HPLC accurate MS, as described below.

The oxidation reaction conditions for 10 µM scopoletin were the same as for scoparone and isoscopoletin (above), except that the 100 µL reaction mixture fluorescence was monitored every 2 min for 40 min using an EnVision 2104 multilabel reader (Perkin Elmer) equipped with filters for excitation at 405 nm and emission at 460 nm. Different amounts of scopoletin (0–10 µM) were used as the standard for calculating the amount of scopoletin consumed during the oxidation reaction. The concentration of scopoletin decreased during incubation and the rate of this decrease was obtained from the slope of the linear phase of concentration decrease versus time. The decrease was dependent on the amount of catalytic enzyme (**Fig. 1S**, Supporting Information).

## Glucuronidation of isoscopoletin and scopoletin

The glucuronidation reactions of 10 µM isoscopoletin were carried out in a total volume of 100 µL, containing 100 mM Tris-HCl buffer (pH 7.4), 5 mM $MgCl_2$, 0.15–0.5 g/L UGT enzyme or 0–0.2 g/L microsomal protein control and 1 mM UDP-glucuronic acid at 37 °C. When the enzyme source were microsomes of different origin, 2.5 mg/L alamethicin was added. The blank reactions lacked ei-

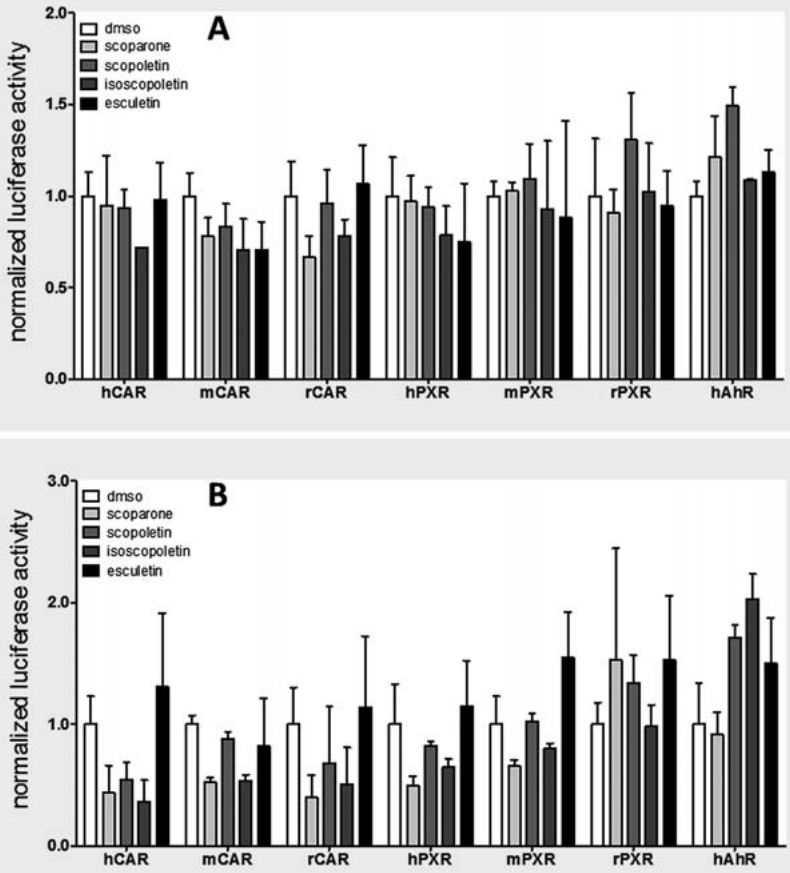


▶ **Fig. 9** Activation of CAR, PXR, and AhR receptors by scoparone and its metabolites scopoletin, isoscopoletin, or esculetin in C3A cells with 10 µM (**A**) and 50 µM (**B**) test concentrations. The data (normalized luciferase activity) are expressed as fold activity over vehicle control (DMSO set at 1) and are means ± SD of 2 independent experiments, both with 3 biological replicates. Positive controls: hCAR 1 µM CITCO (14 ± 0.9), mCAR 1 µM TCPOBOP (11 ± 1.0), rCAR 4 µM clotrimazole (10 ± 3.3), 10 µM androstenole was used to lower basal activity levels, hPXR 10 µM rifampicin (21 ± 4.8), mPXR 10 µM RU486 (2.0 ± 0.2), rPXR 10 µM PCN (54 ± 5.4), and hAhR 10 µM omeprazole (6.8 ± 2.0).

▶ **Table 4** A comparison of human hepatic in vitro scoparone metabolic parameters with the corresponding values from 5 other species. Explanation of symbols: = means similar, + means higher than human, – means lower than human. Number of + or – indicate extent of increased or decreased relative difference, respectively.

| Metabolic parameter | Dog | Pig | Mouse | Rabbit | Rat |
|---|---|---|---|---|---|
| Scoparone oxidation rate | = | + | + | + | – |
| Isoscopoletin/scopoletin ratio | = | = | – | – | – |
| Isoscopoletin oxidation rate | + | ++ | ++ | ++ | – |
| Scopoletin oxidation rate | – | = | = | – | – |
| Isoscopoletin glucuronidation rate | = | ++ | + | ++ | – |
| Scopoletin glucuronidation rate | – | + | + | + | – |

ther isoscopoletin, enzyme, or UDP-glucuronic acid. Samples were incubated for 30 min at 37 °C, and the reactions were stopped by the addition of 300 µL acetonitrile and centrifuged for 5 min 10 000 *g*. The supernatant was stored at − 80 °C and analyzed by HPLC accurate MS as described below.

Scopoletin (10 µM) glucuronidation assay was carried out in the same way, except that the decrease in scopoletin concentration was monitored by fluorescence every 2 min for 40 min. An example of decrease in scopoletin fluorescence that depended on incubation time and amount of UGT enzymes is presented in **Fig. 2S** (Supporting Information).

## Sulfonation of isoscopoletin and scopoletin

The qualitative standards of isoscopoletin and scopoletin sulfate were prepared in sulfonation reactions of 10 µM isoscopoletin or scopoletin in a total volume of 100 µL, containing 100 mM Tris-HCl buffer (pH 7.4), 5 mM $MgCl_2$, 0.3 g/L pig liver cytosol, and 10 µM PAPS at 37 °C. The blank reactions lacked isoscopoletin or scopoletin.

## Scoparone metabolism in humans in vivo

Scoparone solution for the *in vivo* experiment was prepared by mixing 5 mg scoparone in 200 mL water. Two of the authors (HR and ROJ) ingested the solution after which urine samples were collected for 24 h. The 5 mg dose was considered perfectly safe taking into consideration the safety data of scoparone-containing Yin Chen Hao and the parent molecule coumarin. Prior to taking the scoparone solution, control urine samples were collected (blank samples). The urine samples were stored at − 20 °C before analysis. An aliquot of 1 mL urine was centrifuged (14,000 rpm, 5 min, 4 °C) and 100 µL of the supernatant was diluted 1 : 5 in methanol. The samples were filtrated through PALL acrodisc CR 13 mm syringe filter with a 0.2-µm PTFE membrane. The urine samples were measured by HPLC-MS in full-scan mode, in both positive and negative ionization mode. The samples were analyzed in MS/MS using 20 V and 40 V collision energies.

## HPLC accurate MS analysis

Ten micromoles per liter scoparone was incubated in 100 mM Tris-HCl buffer (pH 7.4) containing mouse liver microsomes and the NADPH regenerating system. 150 µL aliquots were taken at 0–40 min to 450 µL acetonitrile. Samples were centrifuged at 10 000 *g* for 10 min, and the supernatant was analyzed with fluorometer as described above and by HPLC-quadrupole time-of-flight (qTOF)-MS (Agilent Technologies) consisting of a 1290 Binary LC system, a Jet Stream ESI source, and a high resolution 6540 qTOF mass spectrometer using positive electrospray ionization mode.

Autosampler tray was kept at 4 °C at all times. For the analyses, 2 µL of the sample solution was injected on a Zorbax Eclipse XDB-C18 column (2.1 × 100 mm, 1.8 µm; Agilent Technologies). Column temperature was 50 °C. Mobile phase flow rate was 0.4 mL/min and consisted of water (eluent A; Milli-Q Gradient (Millipore) and methanol (eluent B; methanol Riedel-de-Häen), both containing 0.1 % v/v of formic acid (Sigma-Aldrich), delivered with the following gradient conditions: 0–10 min: 2 → 100 % B, 10–15 min: 100 % B, 15–15.1 min: 100 → 2 % B; 15.1–18 min: 2 % B.

For chromatographic methods, electrospray ionization source was operated using the following conditions: drying gas (nitrogen) temperature 325 °C and flow 10 L/min, sheath gas temperature 350 °C and flow 11 L/min, nebulizer pressure 45 psi, capillary voltage 3500 V, nozzle voltage 1000 V, and fragmentor voltage 100 V. Data acquisition was performed using 2 GHz extended dynamic range mode across a mass range of *m/z* 50–1600. Scan rate was 2.5 Hz. Data acquisition was in centroid mode with an abundance threshold of 150 counts.

Continuous mass axis calibration was performed by monitoring 2 reference ions from an infusion solution throughout the runs (m/z 121.050873 and m/z 922.009798). Data were acquired using MassHunter Acquisition B.04.00 (Agilent Technologies).

## Activation assay for human and rodent nuclear receptors

C3A cells (ATCC CRL-10741) were grown on 100 mm plates (Corning) in DMEM medium (Gibco 11880), complemented with 10 % FBS (Biowest), 1 % L-glutamine (Euroclone) and 100 U/mL penicillin + 100 µg/mL streptomycin (Euroclone) at 37 °C. For the induction experiments, the cells were transferred onto 96-well plates at a density of $0.156 \times 10^6$ cells per $cm^2$ and cultured overnight. The cells were transfected for 4 h with the previously described plasmid constructs CMX-GAL4-NRLBD (150 ng/well), UAS4-tk-luciferase (100 ng/well), and pCMV$\beta$ (200 ng/well) for other nuclear receptors, or with the human AhR (hAhR)-responsive CYP1A1 promoter driven luciferase (60 ng/well) and pCMV$\beta$ (200 ng/well) [38]. After transfection, the medium was replaced with fresh DMEM medium, complemented with 5 % serum (Biowest) and including either vehicle control (0.1 % DMSO), receptor-activating reference compounds (▶ **Fig. 9**), or test chemicals at 10 µM and 50 µM concentrations, using 3 replicate wells per treatment. To reduce the high basal activity of rCAR, 10 µM androstenole (98 % purity, Sigma-Aldrich) was used. After 24-h treatment, the luciferase and $\beta$-galactosidase activities were measured from 20 µL of the cell lysate as previously described [38]. All luciferase activities were normalized to $\beta$-galactosidase activities and the results are expressed as mean fold ± standard deviation (SD) of 2 independent experiments.

## Supporting Information

MS/MS spectra of scoparone metabolites and data on scopoletin 6-O-demethylation and scopoletin glucuronidation assays are available in the supporting information.


## Acknowledgements

We acknowledge Roche Postdoc Fellowship (RPF) program for providing the dog liver samples. Ms Hannele Jaatinen provided expert technical assistance.


## Conflict of Interest

The authors declare no conflicts of interest.

## References


[1] Hung HY, Kuo SC. Recent studies and progression of Yin Chen Hao (茵陳蒿 Yīn Chén Hāo), a long-term used traditional Chinese medicine. J Tradit Complement Med 2013; 3: 2–6

[2] Jang E, Kim BJ, Lee KT, Inn KS, Lee JH. A survey of therapeutic effects of *Artemisia* capillaris in liver diseases. Evid Based Complement Alternat Med 2015; 2015: 728137

[3] Li JY, Cao HY, Sun L, Sun RF, Wu C, Bian YQ, Dong S, Liu P, Sun MY. Therapeutic mechanism of Yīn-Chén-Hāo decoction in hepatic diseases. World J Gastroenterol 2017; 23: 1125–1138

[4] Wang Y, Wang M, Chen B, Shi J. Scoparone attenuates high glucose-induced extracellular matrix accumulation in rat mesangial cells. Eur J Pharmacol 2017; 815: 376–380

[5] Yamahara J, Kobayashi G, Matsuda H, Katayama T, Fujimura H. The effect of scoparone, a coumarin derivative isolated from the Chinese crude drug *Artemisiae capillaris* flos, on the heart. Chem Pharm Bull (Tokyo) 1989; 37: 1297–1299

[6] Choi BR, Kim HK, Park JK. Penile erection induced by scoparone from *Artemisia capillaris* through the nitric oxide-cyclic guanosine monophosphate signaling pathway. World J Mens Health 2017; 35: 196–204

[7] Jang SI, Kim YJ, Lee WY, Kwak KC, Baek SH, Kwak GB, Yun YG, Kwon TO, Chung HT, Chai KY. Scoparone from *Artemisia capillaris* inhibits the release of inflammatory mediators in RAW 264.7 cells upon stimulation cells by interferon-gamma Plus LPS. Arch Pharm Res 2005; 28: 203–208

[8] Kim EK, Kwon KB, Lee JH, Park BH, Park JW, Lee HK, Jhee EC, Yang JY. Inhibition of cytokine-mediated nitric oxide synthase expression in rat insulinoma cells by scoparone. Biol Pharm Bull 2007; 30: 242–246

[9] Kim JK, Kim JY, Kim HJ, Park KG, Harris RA, Cho WJ, Lee JT, Lee IK. Scoparone exerts anti-tumor activity against DU145 prostate cancer cells via inhibition of STAT3 activity. PLoS One 2013; 8: e80391

[10] Park S, Kim JK, Oh CJ, Choi SH, Jeon JH, Lee IK. Scoparone interferes with STAT3-induced proliferation of vascular smooth muscle cells. Exp Mol Med 2015; 47: e145

[11] Cho DY, Ko HM, Kim J, Kim BW, Yun YS, Park JI, Ganesan P, Lee JT, Choi DK. Scoparone inhibits LPS-simulated inflammatory response by suppressing IRF3 and ERK in BV-2 microglial cells. Molecules 2016; 21: E1718

[12] Xu M, Cai J, Wei H, Zhou M, Xu P, Huang H, Peng W, Du F, Gong A, Zhang Y. Scoparone protects against pancreatic fibrosis via TGF-$\beta$/Smad signaling in rats. Cell Physiol Biochem 2016; 40: 277–286

[13] Zhang A, Sun H, Wu G, Sun W, Yuan Y, Wang X. Proteomics analysis of hepatoprotective effects for scoparone using MALDI-TOF/TOF mass spectrometry with bioinformatics. OMICS 2013; 17: 224–229

[14] Zhang A, Qiu S, Sun H, Zhang T, Guan Y, Han Y, Yan G, Wang X. Scoparone affects lipid metabolism in primary hepatocytes using lipidomics. Sci Rep 2016; 6: 28031

[15] Liu X, Zhao X. Scoparone attenuates hepatic stellate cell activation through inhibiting TGF-$\beta$/Smad signaling pathway. Biomed Pharmacother 2017; 93: 57–61

[16] Huang W, Zhang J, Moore DD. A traditional herbal medicine enhances bilirubin clearance by activating the nuclear receptor CAR. J Clin Invest 2004; 113: 137–143

[17] Masuyama H, Mitsui T, Maki J, Tani K, Nakamura K, Hiramatsu Y. Dimethylesculetin ameliorates maternal glucose intolerance and fetal overgrowth in high-fat diet-fed pregnant mice via constitutive androstane receptor. Mol Cell Biochem 2016; 419: 185–192

[18] Mehta P, Shah R, Lohidasan S, Mahadik KR. Pharmacokinetic profile of phytoconstituent(s) isolated from medicinal plants – a comprehensive review. J Tradit Complement Med 2015; 5: 207–227

[19] Shi P, Lin X, Yao H. A comprehensive review of recent studies on pharmacokinetics of traditional Chinese medicines (2014–2017) and perspectives. Drug Metab Rev 2018; 50: 161–192

[20] Reichard JF, Maier MA, Naumann BD, Pecquet AM, Pfister T, Sandhu R, Sargent EV, Streeter AJ, Weideman PA. Toxicokinetic and toxicodynamic considerations when deriving health-based exposure limits for pharmaceuticals. Regul Toxicol Pharmacol 2016; 79 (Suppl. 1): S67–S78

[21] Yin Q, Sun H, Zhang A, Wang X. Pharmacokinetics and tissue distribution study of scoparone in rats by ultraperformance liquid-chromatography with tandem high-definition mass spectrometry. Fitoterapia 2012; 83: 795–800

[22] Yang D, Yang J, Shi D, Deng R, Yan B. Scoparone potentiates transactivation of the bile salt export pump gene and this effect is enhanced by cytochrome P450 metabolism but abolished by a PKC inhibitor. Br J Pharmacol 2011; 164: 1547–1557

[23] Mennes WC, Van Holsteijn CW, Timmerman A, Noordhoek J, Blaauboer BJ. Biotransformation of scoparone used to monitor changes in cytochrome P450 activities in primary hepatocyte cultures derived from rats, hamsters and monkeys. Biochem Pharmacol 1991; 41: 1203–1208

[24] Horsmans Y, Desager JP, Harvengt C. Scoparone O-demethylase assay is not useful to differentiate the effects of model inducers of cytochrome P-450 in rabbit and guinea pig liver. Life Sci 1993; 53: PL421–PL426

[25] Witkamp RF, Nijmeijer SM, Mennes WC, Rozema AW, Noordhoek J, Van Miert AS. Regioselective O-demethylation of scoparone (6,7-dimethoxycoumarin) to assess cytochrome P450 activities *in vitro* in rat. Effects of gonadal steroids and the involvement of constitutive P450 enzymes. Xenobiotica 1993; 23: 401–410

[26] Wang X, Lv H, Sun H, Liu L, Sun W, Cao H. Development of a rapid and validated method for investigating the metabolism of scoparone in rat using ultra-performance liquid chromatography/electrospray ionization quadruple time-of-flight mass spectrometry. Rapid Commun Mass Spectrom 2007; 21: 3883–3890

[27] Meyer RP, Hagemeyer CE, Knoth R, Kurz G, Volk B. Oxidative hydrolysis of scoparone by cytochrome P450 CYP2C29 reveals a novel metabolite. Biochem Biophys Res Commun 2001; 285: 32–39

[28] Fayyaz A, Makwinja S, Auriola S, Raunio H, Juvonen RO. Comparison of *in vitro* hepatic scoparone 7-O-demethylation between humans and experimental animals. Planta Med 2018; 84: 320–328

[29] Luukkanen L, Taskinen J, Kurkela M, Kostiainen R, Hirvonen J, Finel M. Kinetic characterization of the 1A subfamily of recombinant human UDP-glucuronosyltransferases. Drug Metab Dispos 2005; 33: 1017–1026

[30] Rautio A, Kraul H, Kojo A, Salmela E, Pelkonen O. Interindividual variability of coumarin 7-hydroxylaton in healthy volunteers. Pharmacogenetics 1992; 2: 227–233

[31] Kaipainen P, Koivusaaari U, Lang M. Catalytic and immunologic comparison of coumarin 7-hydroxylation in different species. Comp Biochem Physiol 1985; 81C: 293–296

[32] Raunio H, Rahnasto-Rilla M. CYP2A6: genetics, structure, regulation, and function. Drug Metabol Drug Interact 2012; 27: 73–88

[33] Heikkinen AT, Friedlein A, Matondo M, Hatley OJ, Petsalo A, Juvonen R, Galetin A, Rostami-Hodjegan A, Aebersold R, Lamerz J, Dunkley T, Cutler P, Parrott N. Quantitative ADME proteomics – CYP and UGT enzymes in the Beagle dog liver and intestine. Pharm Res 2015; 32: 74–90

[34] Kurkela M, Patana AS, Mackenzie PI, Court MH, Tate CG, Hirvonen J, Goldman A, Finel M. Interactions with other human UDP-glucuronosyltransferases attenuate the consequences of the Y485D mutation on the activity and substrate affinity of UGT1A6. Pharmacogenet Genomics 2007; 17: 115–126

[35] Kuuranne T, Aitio O, Vahermo M, Elovaara E, Kostiainen R. Enzyme-assisted synthesis and structure characterization of glucuronide conjugates of methyltestosterone (17 alpha-methylandrost-4-en-17 beta-ol-3-one) and nandrolone (estr-4-en-17 beta-ol-3-one) metabolites. Bioconjug Chem 2002; 13: 194–199

[36] Sneitz N, Court MH, Zhang X, Laajanen K, Yee KK, Dalton P, Ding X, Finel M. Human UDP-glucuronosyltransferase UGT2A2: cDNA construction, expression, and functional characterization in comparison with UGT2A1 and UGT2A3. Pharmacogenet Genomics 2009; 19: 923–934

[37] Kurkela M, Siiskonen A, Finel M, Tammela P, Taskinen J, Vuorela P. Microplate screening assay to identify inhibitors of human catechol-*O*-methyltransferase. Anal Biochem 2004; 331: 198–200

[38] Küblbeck J, Laitinen T, Jyrkkärinne J, Rousu T, Tolonen A, Abel T, Kortelainen T, Uusitalo J, Korjamo T, Honkakoski P, Molnár F. Use of comprehensive screening methods to detect selective human CAR activators. Biochem Pharmacol 2011; 82: 1994–2007